Electrogenic Reactions of Cytochrome *bd*†

Audrius Jasaitis,‡ Vitaliy B. Borisov,§ Nikolai P. Belevich,|| Joel E. Morgan,‡ Alexander A. Konstantinov,§ and Michael I. Verkhovsky*,‡

A. N. Belozersky Institute of Physico-Chemical Biology, Moscow State University, Moscow, Russia, Department of Biophysics, Faculty of Biology, Moscow State University, Russia, and Helsinki Bioenergetics Group, Department of Medical Chemistry, Institute of Biomedical Sciences and Biocentrum Helsinki, University of Helsinki, P.O. Box 8, FIN-00014, Helsinki, Finland

Received May 23, 2000; Revised Manuscript Received September 7, 2000

ABSTRACT: Cytochrome *bd* is one of the two terminal quinol oxidases in the respiratory chain of *Escherichia coli*. The enzyme catalyzes charge separation across the bacterial membrane during the oxidation of quinols by dioxygen but does not pump protons. In this work, the reaction of cytochrome *bd* with O_2 and related reactions has been studied by time-resolved spectrophotometric and electrometric methods. Oxidation of the fully reduced enzyme by oxygen is accompanied by rapid generation of membrane potential ($\Delta\Psi$, negative inside the vesicles) that can be described by a two-step sequence of (i) an initial oxygen concentration-dependent, electrically silent, process (lag phase) corresponding to the formation of a ferrous oxy compound of heme *d* and (ii) a subsequent monoexponential electrogenic phase with a time constant <60 μs that matches the formation of ferryl-oxo heme *d*, the product of the reaction of O_2 with the 3-electron reduced enzyme. No evidence for generation of an intermediate analogous to the "peroxy" species of heme−copper oxidases could be obtained in either electrometric or spectrophotometric measurements of cytochrome *bd* oxidation or in a spectrophotometric study of the reaction of H_2O_2 with the oxidized enzyme. Backflow of electrons upon flash photolysis of the singly reduced CO complex of cytochrome *bd* leads to transient generation of a $\Delta\Psi$ of the opposite polarity (positive inside the vesicles) concurrent with electron flow from heme *d* to heme b_{558} and backward. The amplitude of the $\Delta\Psi$ produced by the backflow process, when normalized to the reaction yield, is close to that observed in the direct reaction during the reaction of fully reduced cytochrome *bd* with O_2 and is apparently associated with full transmembrane translocation of approximately one charge.

Activation of molecular oxygen and its 4-electron reduction to water is a key process in biological energy production in aerobic organisms. In a typical case, this highly exergonic reaction is catalyzed by the terminal oxidases of the respiratory chain. Enzymes of this class accept electrons from various donors, of which cytochrome *c* for cytochrome *c* oxidases (CcO)[1] and lipophilic quinols such as ubi- or menaquinol for quinol oxidases are most common. The majority of the enzymes in this class belong to a family of "heme−copper" oxidases (*1*). The oxygen activation site in these oxidases is a binuclear center comprised of a high-spin heme iron and a closely apposed copper ion.

There is an entirely different class of terminal oxidases widely distributed in the bacterial kingdom but represented so far by a sole representative, a quinol oxidase of a *bd*-type (reviewed in refs *2*−*4*). Actually, most of the bacteria contain two gene clusters coding for homologous but different *bd* cytochromes (see refs *5*−*7* and refs therein), and the products of these genes may be exemplified by cytochromes *bd* purified from *Escherichia coli* (or *Azotobacter vinelandii*) and *Bacillus stearothermophilus*.

In *E. coli*, cytochrome *bd* is one of two terminal quinol oxidases and has been characterized in significant detail (*4*). In contrast to heme−copper oxidases, cytochrome *bd* contains no copper, but there are three hemes: heme b_{558}, which has a relatively low midpoint potential, and hemes b_{595} and *d*, which are both high potential. The enzyme catalyzes oxidation of ubiquinol-8 by molecular oxygen:

$$2Q8H_2 + O_2 = 2Q8 + 2H_2O$$

According to current thinking (*8*), the electron-transfer sequence may be described by

$$\text{quinol} \rightarrow b_{558} \rightarrow b_{595} \rightarrow d \rightarrow \text{oxygen}$$

† This work was supported by grants from The Russian Fund for Basic Research [97-04-49765, 98-04-48847, and 99-04-48095], INTAS−RFBR [Grant 95-1259], The Academy of Finland, The Sigrid Jusèlius Foundation, The University of Helsinki, and Biocentrum Helsinki.

* To whom correspondence should be addressed (e-mail: michael.verkhovsky@helsinki.fi).

‡ University of Helsinki.

§ A. N. Belozersky Institute of Physico-Chemical Biology, Moscow State University.

|| Department of Biophysics, Moscow State University.

[1] Abbreviations: **A**, ferrous oxy species;BTP, bis−tris−propane; CcO, cytochrome *c* oxidase; $\Delta\Psi$, electrical membrane potential; DM, *n*-dodecyl β-D-maltoside; LS, lauryl sarcosinate; **P** side, positive side of membrane (corresponds to outer side in mitochondria and bacteria); **P**, "peroxy" species; **F**, oxoferryl species; LTFF, low-temperature flow-flash; **N** side, negative side of membrane (corresponds to inner side in mitochondria and bacteria); **O**, fully oxidized form of binuclear center; Q8, ubiquinone 8; $Ru(bipy)_3$, tris-(2,2′-bipyridyl)ruthenium(II) chloride hexahydrate; τ, time constant, reciprocal of rate constant, $t_{1/e}$; TMPD, *N*,*N*,*N*′,*N*′-tetramethyl-1,4-phenylenediamine.

10.1021/bi001165n CCC: $19.00
Published on Web 10/21/2000

From a chemical point of view, the reaction appears to be analogous to the one catalyzed by the heme−copper quinol oxidases such as cytochrome bo_3; however, efficiency of energy transduction by cytochrome *bd* is only half that of the heme−copper oxidases (*9*−*11*). In heme−copper oxidases, transfer of the four electrons to oxygen is coupled to translocation of eight charges across the membrane. First, four electrons delivered by cytochrome *c* or quinol from the positively charged **P** side of the membrane combine with four protons coming from the opposite, negatively charged, **N** side to make 2 molecules of water. This amounts to transmembrane separation of four charges by means of a (directly coupled) vectorial chemical reaction as first postulated by Mitchell (*12*). Second, in the course of this reaction, four additional protons are translocated all the way across the membrane (*13*). This second type of electrogenic process is usually referred as proton pumping.

Oxidation of $Q8H_2$ by oxygen as catalyzed by cytochrome *bd* is coupled to generation of membrane potential ($\Delta\Psi$) and ΔpH (*9*, *11*, *14*, *15*). Although it has not been conclusively demonstrated, this process is believed to be associated exclusively with the above-mentioned Mitchellian mechanism based on the vectorial chemistry of the reaction (e.g., see the scheme in Figure 8). The protons released by $Q8H_2$ upon its oxidation by cytochrome *bd* (presumably, by low spin heme *b*) are released to the positive periplasmic side of the membrane while the protons consumed in water formation are taken up from the cytoplasmic **N** side. Accordingly, measurements of H^+/e^- stoichiometry for the protons appearing on the outside of bacterial cells consistently give a value about half of that measured for cytochrome bo_3 (*9*, *11*).

The molecular mechanism of redox-linked charge translocation by cytochrome *bd* is of great interest. First, it is of obvious importance to know how this physiologically significant oxidase works. Second, the *bd*-type oxidase, which is expected to exhibit vectorial oxygen reduction chemistry but no proton pumping, can serve as an interesting natural "control" for the heme−copper oxidases in which the processes involved in translocation of "chemical" and "pumped" protons are intertwined and may be difficult to separate.

Time-resolved studies of membrane potential generation by heme−copper oxidases have been highly useful for elucidation of the electrogenic mechanism of those enzymes. Two different methodologies have been used. In one approach, photochemical electron injection into CcO from Ru(bipy)$_3$ or Ru(bipy)$_3$-modified cytochrome *c* is used to initiate individual steps of the oxidase cycle associated with the transfer of the first, third, and fourth electrons (*16*−*20*).

In the other approach, photolysis of CO is used to initiate the reactions studied. The electrometric cell is enclosed in an air-tight enclosure under CO atmosphere. This allows anaerobic photolysis reactions to be studied. In addition, oxygen-saturated buffer can be injected into the sample cell so that the reaction of the partially or fully reduced enzyme with O_2 can be studied (*21*, *22*); a procedure that is effectively equivalent to the flow-flash method used in spectrophotometric studies of oxidases (*23*).

We have now used the CO photolysis-initiated electrometric method to study the generation of $\Delta\Psi$ by cytochrome *bd* in the reaction of the reduced enzyme with O_2 as well as during electron redistribution after photolysis of CO from the partially reduced enzyme in the absence of O_2. We have extended the single wavelength spectrophotometric flow-flash measurements of Hill et al. (*24*) by using a low-temperature flow-flash (LTFF) technique in which a diode array is used to record a complete spectrum at each time point. We have also studied the reaction of fully oxidized cytochrome *bd* with hydrogen peroxide.

MATERIALS AND METHODS

Plant L-lecithin (20%) from Avanti Polar Lipids (Alabaster, AL) was used for preparation of liposomes and for impregnation of the electrometric measuring membranes. Catalase (from bovine liver), cytochrome *c* (from horse heart), and glucose oxidase (type VII, from *Aspergillus niger*) were all from Sigma (St. Louis, MO). Bovine heart cytochrome *c* oxidase was prepared by a modified Hartzell-Beinert/Baker procedure (*25*, *26*) as described in ref *22*.

Cytochrome bd Oxidase Preparation. The GO 105/pTK1 of *E. coli*, which lacks cytochrome bo_3 and overexpresses cytochrome *bd* (*27*), was kindly provided by the laboratory of R. B. Gennis (University of Illinois at Urbana−Champaign). Cells were grown in 10-L flasks at 37 °C in a medium containing 80 mM potassium phosphate, 2.5 mM sodium citrate, 19 mM ammonium sulfate, 1% tryptone, 0.5% yeast extract, 0.5% casamino acids, 0.01% L-tryptophan, 2% glycerol (v/v), 0.8 mM $MgSO_4$, 0.18 mM $FeSO_4 \cdot 7H_2O$, 0.1 mM $CuSO_4 \cdot 5H_2O$, 0.005% kanamycin, and 0.01% ampicillin, pH 7.2. The harvested cells were washed twice with 0.17 M NaCl/5 mM potassium phosphate buffer, pH 7.5, and passed through a French press in 20 mM Tris, 5 mM $MgSO_4$, and 0.5 mM EDTA, pH 8.3. Immediately before the French press treatment, the mixture was supplemented with 0.3 mM PMSF and DNAase I (0.01 mg/mL). Intact and partially broken cells were removed by centrifugation at 14500*g* for 15 min at 4 °C. The membranes were sedimented from the supernatant (48000*g*, 60 min, 4 °C) and homogenized in 150 mM KCl, 5 mM EDTA, and 75 mM potassium phosphate buffer, pH 6.5. Cytochrome *bd* was isolated from the membranes as described in ref *28* but omitting the final hydroxylapatite chromatography step. Its concentration was determined as in ref *29* from the dithionite-reduced minus air-oxidized difference absorption spectra using a value of $\Delta\epsilon_{628-607}$ of 10.8 mM^{-1} cm^{-1}, which corresponds to $\Delta\epsilon_{561-580} = 21$ mM^{-1} cm^{-1} in ref *30*.

Reconstitution of Enzymes into Phospholipid Vesicles. Liposome reconstitution of bovine aa_3 oxidase was performed as described in ref *22* using a procedure based on the cholate/Biobeads (Bio-Rad) method of Rigaud et al. (*31*). Cytochrome *bd* oxidase was reconstituted using essentially the same procedure used earlier for cytochrome bo_3 oxidase (*32*) except that dilution of liposomes and washing from the buffer steps were omitted. For some experiments where fast re-reduction of cytochrome *bd* oxidase was required, liposomes were prepared containing ubiquinone 8 (Q8) in the lipid milieu. To this end, a 1 mM solution of Q8 in ethanol was mixed with an equal volume of asolectin solution in decane, and the mixture was lyophilized on a vacuum line. The resulting ~1 mM Q8 "solution" in the lipid was used subsequently for the reconstitution procedure.

Spectrophotometric Time-Resolved Measurements at Low Temperature. LTFF measurements were carried out as in ref

33 using a diode array kinetic spectrophotometer made by Unisoku Instruments (Kyoto, Japan). The cuvette containing the CO-inhibited reduced enzyme (cytochrome *bd* in 60 mM HEPES−KOH/25 mM phosphate buffer, pH 7.5, LS (0.025%), DM (0.1%), 40% ethylene glycol, and 1 atm CO) was placed in the cuvette holder, which was then cooled using a Lauda RCS thermostat. The windows were kept dry by a nitrogen flush. Oxygen-saturated buffer (60 mM HEPES−KOH, pH 7.5, and 40% ethylene glycol), also at low temperature, was mixed into the sample (1:1 vol/vol), and the reaction was initiated by a xenon camera flash (Braun 2000/320 BVC). To minimize CO photolysis by the monitoring light prior to the flash, a camera shutter (Olympus OM-10) was used to block the beam until a few milliseconds before the flash. Timing of delays by Metrabyte CTM-05 PC counter-timer board; software written by J.E.M.

Electrometric Time-Resolved Measurements of Membrane Potential Generation. The direct, time-resolved electrical measurement is based on a method originally developed by Drachev and co-workers (*34*, *35*). In the present system, Ag/$AgCl_2$ electrodes record the voltage between the two compartments of a cell separated by a measuring membrane consisting of a lipid-impregnated, stretched Teflon mesh. Vesicles, into which the enzyme has been reconstituted, are forced to associate with this measuring membrane (see Figure 2 in ref *21*). The voltage across the measuring membrane follows the $\Delta\Psi$ across the vesicle membranes proportionally, allowing the kinetics of charge translocation to be recorded. The method is described in more detail in refs *21* and *22*.

Electrometric Measurements Involving Dioxygen. Flow-flash type measurements require O_2-saturated buffer to be introduced into the sample shortly before the photolysis flash. In the electrometric apparatus, this O_2-saturated buffer was delivered through a long narrow needle positioned so that the jet from the needle was directed at the measuring membrane (a 4 mm circle) in order to produce a high local concentration of oxygen for the time of the reaction (see Figure 2 in ref *21*). A computer-driven syringe pump (SP200i, World Precision Instruments) with a 2.5-mL gas-tight syringe was used. Portions of 100 μL of O_2-saturated buffer were injected (5 mL/min) via a 450-mm 22S gauge RN needle (Hamilton, Reno, NV). The reaction was initiated by a flash from a frequency-doubled YAG laser (Quantel Brilliant, pulse energy 180 mJ).

Spontaneous CO dissociation from heme *d* is relatively fast ($k = 1.6\ s^{-1}$; *24*) while delivery of the entire 100 μL of oxygenated buffer takes about 1.2 s. This means that the enzyme can begin to react with O_2 before the flash. To avoid this loss of starting material, the laser was fired before the oxygen injection had ended, typically 450 ms after the start of the injection. However if the delay is too long, the amplitude of the photoinduced reaction decreases (not shown). (Note that the flash-induced reaction is a single turnover and is complete within few milliseconds; therefore, changes of oxygen concentration during the actual reaction can be neglected.)

Microsecond Transient Absorbance Measurements. Flash-induced rapid spectrophotometric measurements were carried out as described previously (*36*). Two channel (sample/reference) data digitization was done with a CompuScope 512 12-bit PC card (Gage Applied Sciences, Montreal, Canada) running data acquisition software, written by N.P.B. Samples were place in rectangular fluorescence-type cuvettes (5 optical windows) with internal dimensions of 4 × 10 mm, equipped with joints for attachment to the vacuum line. As prepared, aerobic cytochrome *bd* has O_2 bound to reduced heme *d*. To prepare the CO mixed-valence form of the enzyme, it was first necessary to remove this bound O_2. This was done by repeatedly "washing" the sample with argon; using the vacuum/gas line, the atmosphere in the cuvette was replaced with oxygen-free argon, and the cuvette was then gently rocked to equilibrate the sample with the new atmosphere. After several such cycles, removal of oxygen from heme *d* could be observed by a shift of heme *d* absorbance from 640 to 632 nm. Carbon monoxide was then introduced into the sample to form the single-electron reduced CO-bound form of the enzyme. This was done by using the vacuum/gas line to replace the atmosphere in the cuvette with a gas mixture of 1% CO and 99% argon.

RESULTS

Spectrophotometric Studies of the Reaction of Reduced Cytochrome bd with Dioxygen. The reduction of O_2 by cytochrome *bd* includes intermediates whose lifetimes are measured in microseconds. This is much too fast to be studied by conventional mixing methods, which have only millisecond resolution. This limitation can be overcome if the reaction is started by a flash of light rather than by mixing. To do this, carbon monoxide is used to "cage" the enzyme while O_2 is mixed into the sample. After being mixed, CO can be removed by a flash of light. In less than 1 μs the flash creates the initial reaction conditions—the unliganded, fully reduced enzyme in the presence of oxygen—in the whole sample. In effect, this synchronizes the sample, so that the entire enzyme population becomes available for the reaction within a single sub-microsecond window. This coherent start makes it possible, as the reaction goes forward, for intermediates with very short lifetimes to be resolved. The technique, known as flow-flash, was originally developed by Gibson and Greenwood in 1963 for use with cytochrome *c* oxidase and has become an indispensable tool for the study of terminal oxidases.

Fully reduced cytochrome *bd* contains three reducing equivalents, one short of the number needed to reduce O_2 to 2 water molecules. Instead, the immediate end product of the reaction is a ferryl compound (**F**) of cytochrome *d* (*24*). Hill and co-workers (*24*) studied this reaction, recording the time course at individual wavelengths, and found two phases. The first phase was dependent on oxygen concentration at all values measured (rate constant $2 \times 10^9\ M^{-1}\ s^{-1}$) and was assigned as the binding of oxygen to heme *d* to form a ferrous oxy species (**A**). The second phase was independent of oxygen at concentration above 50 μM (rate constant $1.3 \times 10^4\ s^{-1}$) and was assigned as conversion of ferrous oxy heme *d* to an oxy-ferryl (**F**) with simultaneous oxidation of low-spin heme *b*.

To explore this reaction in more detail, we repeated the experiment using a low-temperature version of the flow-flash method in which the reaction is carried out at about −20 °C (in an antifreeze solution) in order to slow it down to the point where the millisecond resolution of a diode array can adequately capture kinetics of the process (*33*). This makes it possible to obtain a complete spectrum of the sample (500−700 nm) every millisecond as the reaction unfolds.

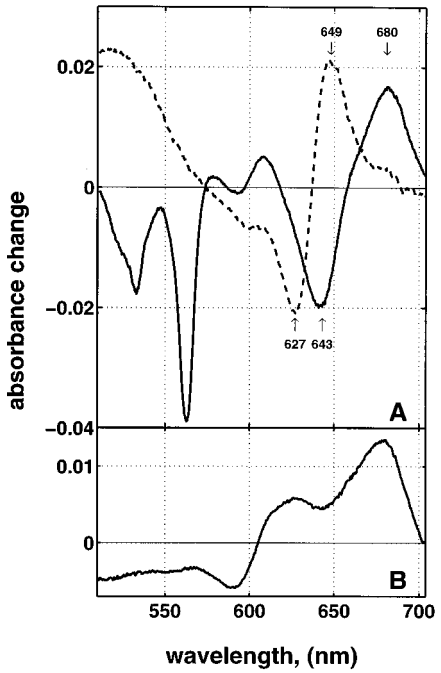

FIGURE 1: Optical spectra of kinetic components from (A) low-temperature flow-flash and (B) room temperature peroxide reactions. (A) Reaction of O_2 with fully reduced cytochrome *bd* at −20 °C; components from global multiexponential fit. Rates: dashed line, $k = 1250\ s^{-1}$; solid line, $k = 130\ s^{-1}$. Cytochrome *bd* in HEPES−KOH, 60 mM; phosphate buffer, 25 mM (pH 7.5); LS, 0.025%; DM, 0.1%; ethylene glycol, 40%; 1 atm CO) was cooled in the spectrophotometer. An equal volume of O_2-saturated buffer HEPES−KOH, 60 mM (pH 7.5); ethylene glycol, 40%, also at low temperature, was mixed into the sample prior to the flash. (B) Single kinetic component from stopped-flow reaction of H_2O_2 with the fully oxidized cytochrome *bd* at room temperature; one of the two syringes contained air-free oxidized cytochrome *bd* (ca. 8 μM in HEPES−KOH, pH 7.5, 0.1% Tween 20, and 100 μM ferricyanide). The other syringe contained 20 mM H_2O_2 in the same buffer. Mixing ratio 1:1.

When fully reduced cytochrome *bd* reacts with dioxygen in the LTFF experiment, evolution of absorption changes begins immediately after the flash and reaches completion within about 100 ms. Global analysis of the surface of spectra collected during the reaction reveals two clear transitions (Figure 1) in agreement with Hill et al. (*24*). At −20 °C, the two phases have time constants of ≤1 and 7.7 ms. The spectrum of the first phase has a peak at 650 nm and a trough at 630 nm, typical of π-donor ligand binding to reduced heme *d*, as expected for formation of the **A** intermediate (Figure 1, dashed line). In addition, there may be some perturbation of the ferrous heme b_{595} spectrum as evidenced by minor absorption changes around 600 nm.

When cytochrome *bd* is prepared, there is typically a population of the enzyme in which heme *d* is reduced with O_2 bound, i.e., a ferrous-oxy species (**A**). The bound O_2 can be removed by repeatedly exchanging the gas atmosphere of the sample with air-free argon (see Materials and Methods). To obtain a reference spectrum of **A**, the spectral changes that accompany removal of O_2 were measured. In the spectral region from 620 to 700 nm, this difference spectrum is almost exactly the inverse of the spectrum of the first phase of the O_2 reaction (Figure 1). This supports the assignment of this kinetic phase as O_2 binding to reduced heme *d*. There are larger differences in the spectral region from 520 to 620 nm. This reflects electron redistribution in the argon-exchanged sample after O_2 is removed from heme *d*, a process analogous to "electron backflow" after photolysis of CO (below).

The ferrous oxy intermediate (**A**) then decays in a monoexponential process to a state with increased absorption at 680 nm. There is simultaneous oxidation of heme b_{558} (the troughs at 560 and 530 nm are the α- and β-bands, respectively). The 680 nm feature has been assigned to the **F** state of the enzyme on the basis of resonance Raman spectra (*37*, *38*). It is thought that heme b_{595} also becomes oxidized in this phase, although it is possible that the small trough at 595 nm may be accounted for as part of the heme *d* ferryl-oxo spectrum (cf. lower panel, Figure 1; see below). The reaction stops at this point—with O_2 reduced to the 3-electron level. The spectra of the two phases confirm the assignments of Hill et al. (*24*). However, the time constants are not comparable because of the ∼40 °C temperature difference between the two sets of measurements.

In cytochrome *bd* the **A** intermediate appears to decay directly to the **F** state. In contrast, in cytochrome *c* oxidase (aa_3) an intermediate known as **P** intervenes between these two states and is clearly resolvable under conditions similar to those of the present measurements (*33*). However, there are no indications of an analogous intermediate in the present data.

Generation of Membrane Potential Coupled to the Reaction of Reduced Cytochrome bd with Dioxygen. The biologically significant product of the cytochrome *bd* reaction is energy. The energy output of the enzyme goes to create and maintain an electrochemical membrane potential ($\Delta\mu_{H+}$), which serves as a power source for the cell. Drachev and co-workers (*34*, *35*) developed method by which the growth of potential across the membrane ($\Delta\Psi$) can be followed on a sub-microsecond time scale by electrical measurements. Originally used for photosynthetic (*39*) and bacteriorhodopsin work (*40*), this "electrometric" technique has recently been applied to time-resolved studies of the heme−copper oxidases. One method employs photoreductants, such as Ru(bipy)$_3$, to inject electrons into the enzyme (*16*, *20*, *41*). This cannot be applied to cytochrome *bd* because suitable photoreductants are not available. A second method duplicates the conditions of the classical flow-flash technique (*23*) but with the enzyme in vesicles that are attached to a stationary measuring membrane (see Materials and Methods). This method has now been used to study cytochrome *bd*.

These electrometric measurements depend on net charge movement in the membrane, which cannot be observed if the working enzyme population is equally divided between outside-out and inside-out orientations. To avoid random orientation, cytochrome *bd* was reconstituted into vesicles using a new method developed by Rigaud et al. (*31*), which has been shown by Verkhovskaya et al. (*32*) to give good results with cytochrome bo_3 of *E. coli*.

The reaction of reduced cytochrome *bd* with O_2 produces a membrane potential, which is negative inside the vesicles. (This is equivalent to negative inside the cell.) A typical recording is shown in Figure 2. After the flash, there is a small but reproducible lag phase (inset) after which the electrogenic response rises in a single-exponential phase with a rate of $1.7 \times 10^4\ s^{-1}$ ($\tau \sim 60\ \mu s$). The kinetics of the response can be modeled reasonably well by a linear reaction

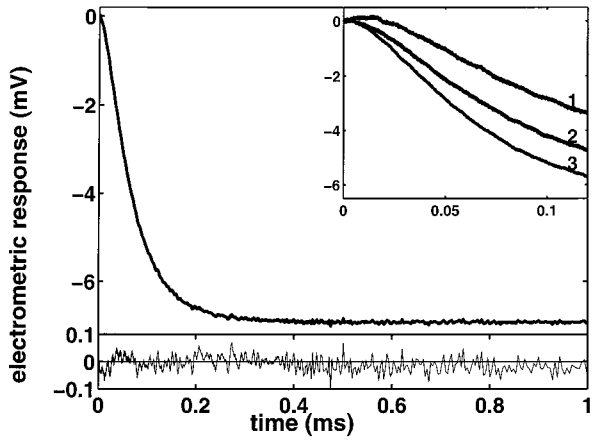

FIGURE 2: Development of membrane potential during the reaction of fully reduced (three electrons) cytochrome *bd* with oxygen. Main panel: a typical data recording; bottom panel, difference between experimental and theoretical curves; inset, the early part of the reaction with three different delays between start of injection and laser flash. Conditions for the main panel: 100 mM HEPES−KOH, pH 8, 10 μM TMPD, 50 mM glucose, 50 μg/mL catalase, 130 μg/mL glucose oxidase, and 1% CO mixture with Ar. Reaction started after 450 ms from the beginning of injection of 100 μL of oxygen-saturated buffer ([O_2] = 1.2 mM). The fit gives the following parameters for the two phases in the model curve: **R**→**A**, $k = 6.6 \times 10^4$ s^{-1}, amplitude, 0 (i.e., the phase is nonelectrogenic); **A**→**F**, $k = 1.7 \times 10^4$ s^{-1}, amplitude, −6.9 mV. Inset: the laser flash was delivered at (1) 325, (2) 400, and (3) 450 ms after start of oxygen additions; other conditions are the same.

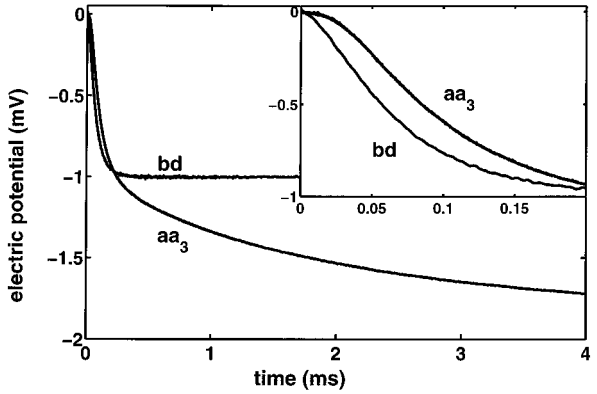

FIGURE 3: Comparison of electrometric time courses for the reaction with O_2 of cytochrome *bd* from *E. coli* and bovine CcO. The traces have been normalized to the amplitude of the ∼100 μs electrogenic phase. Inset: first 200 μs of the reaction. Conditions: for cytochrome *bd* as in Figure 2; for CcO same but with additions of the following redox mediators: cytochrome *c*, 0.5 μM; hexaamineruthenium, 10 μM; TMPD, 100 μM; DCPIP, 100 μM; ferrocyanide, 60 mM.

sequence A→B→C where A→B is electrically silent (*22*). Increasing number of intermediates does not improve the fit (see plot of residuals in the lower panel of Figure 2).

These two reaction steps match neatly with the two phases found in the spectrophotometric experiments (ref *24* and above). The appearance of the first phase in the electrometric data (A→B) as a lag is consistent with its assignment as an oxygen binding process. This is reminiscent of what has been seen in the heme−copper oxidases, where the binding of oxygen is not electrogenic (*22*). The major electrogenic phase (B→C; $\tau \sim 60$ μs) corresponds well with the second phase reported by Hill and co-workers (*24*) ($\tau \sim 80$ μs). The ∼1.3-fold difference between these values is probably not significant; even though the conditions of the experiments were slightly different in temperature (24−25 vs 20 °C) and enzyme environment (lipids vs detergent), the difference in the rates appears to be within the uncertainty of the spectrophotometric measurements (Figures 3 and 4 in ref *24*). There is a significant H_2O to D_2O solvent isotope effect on the major electrogenic phase; the fitted time constant increases from 60 to 230 μs. There is no discernible effect on the lag.

As described in Materials and Methods, spontaneous CO dissociation from heme *d* is fast enough to compete with the introduction of oxygen-saturated buffer into the sample. The time constant for CO dissociation is about 600 ms while the complete injection takes 1.2 s. For this reason the reaction had to be initiated before the injection was complete, and the O_2 concentration never reached the levels typically used for spectrophotometric flow-flash experiments. As shown in Figure 2 (inset), increasing the delay between the start of oxygen injection and CO photolysis from 300 to 450 ms resulted in a marked reduction of the initial lag. The longer delay allows more O_2 to enter the sample, shortening the lag. This is qualitative confirmation of the results of Hill et al. (*24*) that the initial phase of the reaction depends on the oxygen concentration. At the highest oxygen concentrations that could be delivered to the reaction zone, the time constant for the lag phase was 15 μs. Using the bimolecular rate constant of Hill et al. (*24*) of 2×10^9 M^{-1} s^{-1}, this would correspond to [O_2] ∼ 33 μM. The rate constant of the major electrogenic phase showed only a modest dependence on the O_2 concentration.

It is instructive to compare the kinetics of $\Delta\Psi$ generation by cytochrome *bd* and bovine CcO (*22*) (Figure 3). The major 60 μs electrogenic phase in the cytochrome *bd* oxygen reaction can be seen to have a closely matching counterpart in the electrogenesis revealed by cytochrome aa_3 identified earlier as the $\mathbf{P}_R$ to **F** transition (*22*). There are however two clear distinctions between the enzymes:

First, in the reaction of CcO with O_2, the development of $\Delta\Psi$ includes an additional phase that evolves on a millisecond time scale. This is explained by the fact that, although fully reduced cytochrome *bd* carries only three reducing equivalents, CcO carries four. The reaction of fully reduced cytochrome *bd* with dioxygen stalls at **F** stage, but in CcO the presence of a 4th electron allows the reaction to continue one step past **F** to produce water, together with the fully oxidized enzyme.

Second, in case of CcO the lag phase is much more pronounced (Figure 3, inset). To fit the CcO $\Delta\Psi$ generation data, at least two sequential nonelectrogenic or weakly electrogenic steps preceding the ∼100 μs electrogenic phase must be included in the model. As discussed in ref *22*, these steps correspond to binding of oxygen to the reduced enzyme (**R**→**A** transition) and conversion of the **A** intermediate to the **P** intermediate (**A**→**P**). A similar lag is observed in the reaction of the bo_3-type quinol oxidase from *E. coli* (A. Jasaitis and M. I. Verkhovsky, unpublished results). In cytochrome *bd* the lag is much shorter and, as mentioned above, can be fitted by a single step in the kinetic model. This supports the conclusion from the spectrophotometric measurements (ref *24* and above) that in cytochrome *bd* intermediate **A** decays directly to **F**. In contrast to the heme−copper oxidases, in the reaction of cytochrome *bd* with O_2

there is either no **P** intermediate or this intermediate is too short-lived to be detected.

Reaction of the Oxidized Cytochrome bd with Hydrogen Peroxide. Another possible way to generate **P** in cytochrome *bd* is by reaction with hydrogen peroxide. H_2O_2 is known to react with heme−copper oxidases to produce **P** and/or **F** depending on conditions (*42*−*46*). When the reaction of H_2O_2 with cytochrome *bd* was originally studied, two spectrally different peroxide complexes were reported, but one of the two was only found when the reaction began with the "oxygenated" enzyme (*47*). If the reaction is started from the homogeneous oxidized state, only one spectral intermediate, **F**, is generated (*47*, *48*).

In CcO, **P** is easily converted to **F** by excess peroxide (*43*, *45*, *46*, *49*, *50*). In cytochrome *bd* the possibility remained that **P** was formed transiently during the reaction with excess peroxide but had escaped observation in previous studies (*38*, *47*, *48*). For example, in cytochrome bo_3 (a quinol oxidase), it was originally believed that reaction with peroxide proceeded directly to **F** (*51*−*53*). **P** was only identified as an intermediate in this reaction when favorable conditions were found, and the reaction was studied by means of a stopped-flow spectrophotometer with a millisecond diode array, which allowed the evolution of the entire spectrum to be followed (*50*, *54*).

To investigate this possibility, the reaction of oxidized cytochrome *bd* with H_2O_2 was repeated under the same conditions where **P** had been identified in cytochrome bo_3. However, in contrast to the aa_3 and bo_3 oxidases, in cytochrome *bd* the peroxide reaction is monophasic (τ = 700 ms). The difference spectrum for the single kinetic phase (Figure 1B) is identical to that of the final product formed upon addition of excess hydrogen peroxide to ferric cytochrome *bd* (*38*, *47*, *48*), which has been assigned to the **F** species (*37*). There is thus no evidence for an intermediate corresponding to **P** of heme−copper oxidases in the electrometric or spectrophotometric studies of the reaction of O_2 with reduced cytochrome *bd* or in the reaction of H_2O_2 with the oxidized enzyme.

Investigations of Internal Electron Redistribution in Cytochrome bd. The reactions studied in the flow-flash experiment are complicated processes that involve electron transfer, O_2 redox chemistry, proton uptake for water formation, and, in the case of heme−copper oxidases, proton translocation. In trying to understand such a complicated process, it can be helpful to study a simpler part of the whole. In the case of terminal oxidases, one simplification is to study internal electron transfer/redistribution in the enzyme in the absence of O_2. This has been done in a number of different ways, but one method that has proved to be very useful is to prepare a CO-bound mixed-valence state of the enzyme and to observe electron redistribution after photolyzing CO, a process known as electron backflow (*36*, *55*−*59*).

Junemann et al. (*60*) have reported electron backflow in cytochrome *bd* of *Azotobacter vinelandii*. They prepared a one-electron reduced form of the enzyme with CO bound to heme *d* (b_{558}^{3+}, b_{595}^{3+}, d^{2+}-CO), and found that when CO was photolyzed there was electron redistribution from heme *d* to heme(s) *b*. These experiments were done in the presence of aurachin D, which raises the E_m of heme b_{558} making it a better electron acceptor. After the experimental conditions were optimized, we were able to spectrophotometrically resolve the corresponding phenomenon in solubilized cytochrome *bd* from *E. coli* even in the absence of aurachin D.

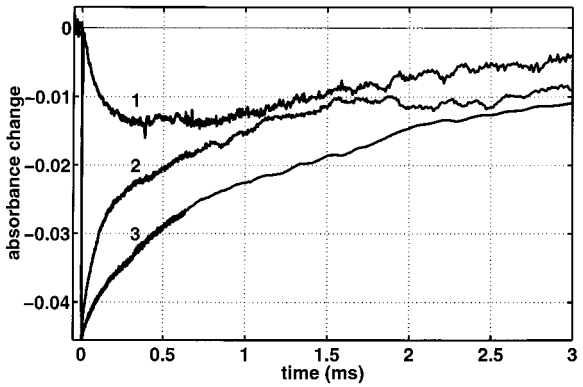

FIGURE 4: Time course of electron backflow in mixed-valence cytochrome *bd* recorded spectrophotometrically at various wavelengths: (1) 634, (2) 562, and (3) 642 nm. Conditions: cytochrome *bd* oxidase, 10 μM; DM, 0.1%; HEPES−KOH, 100 mM (pH 8); CO, 1%; light path, 1 cm.

Figure 4 (trace 1) shows the redox changes in heme *d* measured at 634 nm. CO photolysis makes almost no contribution at this wavelength (there is no initial jump). The subsequent process is essentially monophasic oxidation of heme *d* with a time constant of ca. 150 μs. Theses changes return monophasically with the time constant of 1.3 ms, in agreement with the expected rate of CO rebinding at 1% saturation (trace 3).

At 562 nm (the α-band maximum for low-spin heme b_{558} in the reduced-oxidized difference spectrum, trace 2), the flash brings about an immediate loss of absorbance due to the contribution of CO photodissociation from heme *d* at this wavelength, which agrees with the data in ref *60*. Notably, return of absorbance to the initial level in this case is not homogeneous (cf. trace 3) but reveals an initial rapid phase of A_{562} increase with τ of ∼150 μs concomitant with the oxidation of heme *d* as measured at 634 nm (trace 1). Apparently, this rapid phase reports reduction of heme b_{558} overlapping the slow decay of the response associated with contribution of heme *d* recombination with CO (trace 3).

If the 150 μs phase of heme *b* reduction is attributed solely to b_{558}, the amplitude of the response would correspond to ∼4% of this redox center, in good agreement with the 4% of heme *d* oxidized, as calculated from the spectrophotometric trace at 634 nm. In fact, the electron is likely to be shared between hemes b_{558} and b_{595}, which make comparable contributions to absorbance at 562 nm (*61*) and have similar redox potentials (*4*). Therefore, the true value of heme b_{558} reduction will be somewhere between 2 and 4%.

Electrometric Measurements of Electron Backflow in Cytochrome bd. Photolysis of CO from liposome-incorporated mixed-valence cytochrome *bd* under anaerobic conditions results in transient generation of $\Delta\Psi$, which is *positive* inside the vesicles, i.e., with a polarity opposite to that observed during the reaction with O_2. In Figure 5**,** the kinetics of heme *d* oxidation at 634 nm (trace 2) and the flash-induced rise of electric potential difference in the backflow experiments (trace 1) are compared directly. There is excellent agreement between the two traces showing that the reverse membrane potential is associated with the reverse electron flow in mixed-valence cytochrome *bd*. The signal-to-noise ratio of the electrometric trace is clearly superior to that of

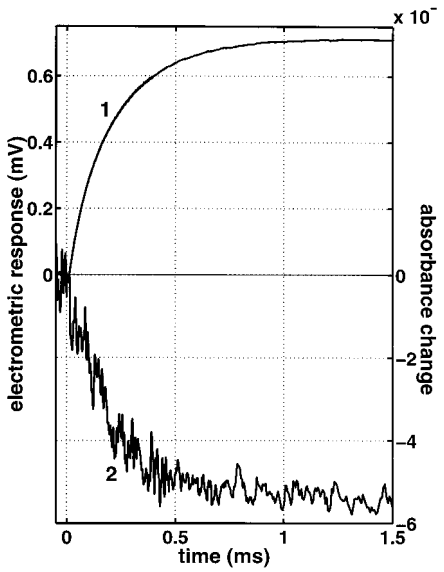

FIGURE 5: Comparison of electron backflow reactions measured by optical spectrophotometry at 634 nm (curve 2, right axis) and by electrometric method (curve 1, left axis). Conditions in the optical experiment as in Figure 4. In the electrometric experiment, as in Figure 2**,** except that no O_2 was added and the enzyme was not allowed to become fully reduced.

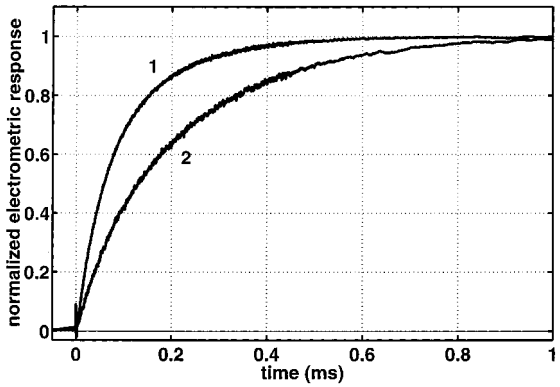

FIGURE 6: Electrometric responses of cytochrome *bd* coupled to electron backflow following CO photolysis from CO mixed-valence enzyme in H_2O and D_2O. Conditions as in Figure 2, except that no O_2 was added and the enzyme was not allowed to become fully reduced.

the absorbance trace. This makes it possible to analyze the kinetics of the backflow process in much more detail than is allowed by the quality of the absorbance measurements. As shown in Figure 6, the electrometric response shows a significant H_2O/D_2O solvent isotope effect. The ratio of rate constants is about 1.5.

Figure 7 shows three electrometric backflow transients obtained at 1%, 10%, and 100% of CO. Higher concentrations of CO result in faster decay of the response, as expected for CO recombination, but the initial rate of the flash-induced rise remains essentially constant. Acceleration of the decay at high CO concentrations is paralleled by a decrease in the amplitude of the response that is a trivial effect of competition between CO recombination and the rising phase. The amplitude of the response slowly decreases with time as the other metal centers in the enzyme become reduced in the anaerobic environment. If the liposome-reconstituted enzyme is incubated for a long time (hours) under an atmosphere of 100% CO, the electrometric response eventually disappears;

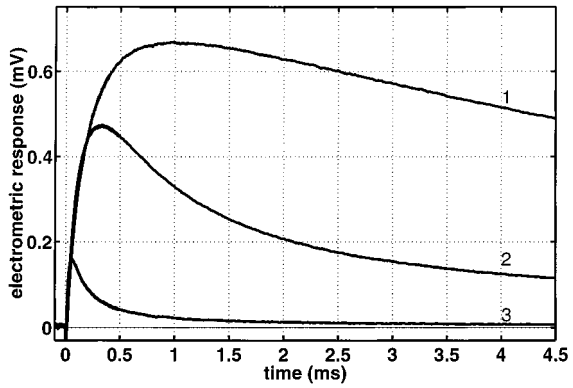

FIGURE 7: Electrometric responses of cytochrome *bd* coupled to electron backflow following CO photolysis from CO mixed-valence enzyme. The CO concentration dependence. Experiments have been carried out varying CO concentrations in the CO/argon gas mixture: (1) 1% CO, (2) 10% CO, and (3) 100% CO.

this disappearance correlates with the reduction of the enzyme in spectrophotometric control experiments with purified cytochrome *bd*. According to our experience, the reducing equivalents come at least partly from the glucose/glucose oxidase system used to maintain the sample in an anaerobic state, and reduction is promoted significantly by illumination of the sample in the course of experiments.

DISCUSSION

Redox Mechanism of Cytochrome bd: No Evidence for Peroxy State. The reaction of cytochrome *bd* with O_2 is usually considered to involve the same intermediates as in the heme−copper oxidases. However, despite all attempts, we were unable to produce, in this enzyme, an intermediate analogous to **P** (the 607 nm species in CcO (*62*) or the 582 nm species in bo_3-type quinol oxidase (*50*, *54*)).

The negative results have been provided by three independent approaches. First, the LTFF measurements of the reaction of reduced *bd* with O_2 clearly resolve initial formation of a **A** intermediate and show that this complex proceeds directly to the final **F** state. Transient of the **P** intermediate ($\mathbf{P}_R$) under these conditions has been documented for CcO (*33*). Second, rapid mixing of oxidized cytochrome *bd* with hydrogen peroxide results in monophasic formation of the **F** state without any intermediate, whereas the same reaction leads to transient formation of **P** in CcO (*43*, *45*) and cytochrome bo_3 (*50*, *54*). Third, the flow-flash electrometric data for cytochrome *bd* are consistent with a simple one-step lag preceding the electrogenic transition of the enzyme to the **F** state rather than the two steps needed to fit the lag in the case of the heme−copper oxidases; this single phase corresponds to formation of the oxy complex of the high-spin heme while the counterpart corresponding to the **A**→**P** transition is absent in cytochrome *bd*. The electrometric experiment is particularly important as it allows us to exclude the possibility that **P** in cytochrome *bd* is spectroscopically similar to the ferryl, oxygenated, or ferric state and thus is not discernible in spectrophotometric measurements. The absence of an observable **P** intermediate in cytochrome *bd* may find its explanation in one of two ways.

One possibility is that an intermediate analogous to **P** is not formed in cytochrome *bd* at all and that the chemistry

of O_2 reduction is different in this enzyme as compared to the heme−copper oxidases. Alternatively, one can propose that the reaction mechanisms are the same but the **P** state in cytochrome *bd* is much less stable than in heme−copper oxidases and is converted rapidly to **F** state both during O_2 reduction and in the reaction of the oxidized enzyme with hydrogen peroxide.

It is worth noting in this context that in cytochromes P-450 and peroxidases the **O** species, which corresponds to the **P** intermediate in the respiratory oxidases (*63*), does not accumulate and is converted in microseconds to a ferryl-oxene state. Babcock and co-workers (*64*, *65*) have noted that the remarkably high stability of **P** in CcO as compared to P-450 may be explained by the **P**→**F** transition being coupled to relatively slow proton pumping. It is tempting to speculate that as cytochrome *bd* does not pump protons, the **P**→**F** transition in this enzyme need not be as slow as in the pumping oxidases and that in this respect cytochrome *bd* resembles P-450 and peroxidases.

Generation of Δψ−vectorial Movement of Electrons and/or Protons? Our data show that the redox reaction between the hemes *d* and b_{558} is coupled to charge movement across the membrane. As illustrated by the scheme in Figure 8, this electrogenicity could originate in electron-transfer per se (panel B) and/or in vectorial transfer of protons coupled to the redox reaction (panel A).

Unlike the heme-copper oxidases (*66*, *67*), no three-dimensional structural model is available for cytochrome *bd*, and what information is available about the spatial arrangement of its redox centers is not definitive. Hemes b_{595}/*d* and heme b_{558} were earlier believed to be located on opposite sides of the membrane, b_{558} close to the **P** side and the b_{595}/*d* pair close to the **N** side (e.g., cf. Figure 2 in ref *4*). This would mean that transmembrane electron transfer between the hemes (*68*) in cytochrome *bd* oxidase could potentially be a redox loop-type generator of membrane potential as proposed originally by Mitchell for mitochondrial CcO (*69*). This is illustrated in Figure 8B. However, recent re-evaluation of membrane topology predictions for cytochrome *bd* suggest that the axial ligands for both hemes b_{595} and b_{558} are located at about the same depth in the membrane, quite close to the **P** side (*7*). This "electrical topography" appears to be rather similar to that in heme−copper oxidases where electron transfer between the hemes is unlikely to be significantly electrogenic. Therefore, in light of the electrometric results—in particular the H_2O/D_2O solvent isotope effect—the possibility of vectorial proton-transfer coupled to the redox reaction between the hemes *b* and *d* must be considered (Figure 8A).

It should be noted that midpoint potentials of all the three hemes of cytochrome *bd* show pH dependencies indicative of strong, specific electron/proton coupling (*4*). The sidedness of this redox-linked protonation has not been studied, but our data can be most easily rationalized in a following way. During electron flow in the normal direction, heme b_{558}, which interacts with the quinol, accepts both an electron and a proton from QH_2. Upon oxidation of b_{558} by heme *d* (probably via b_{595}), the proton is released to the **P** side, while reduced heme *d* takes up a proton from the **N** side of the membrane. Such an arrangement would lead to translocation of one elementary charge (actually, of a proton) per electron, across the membrane, consistent with cytochrome *bd* not being a proton pump. During reversed electron transfer in the backflow experiments, oxidation of heme *d* would release the redox-dependent proton to the **N** side of the membrane while reduction of heme b_{558} would result in proton uptake from the **P** side, thus giving rise to transmembrane translocation of one charge. The electrometric measurements themselves do not tell us whether the protons actually appear in and/or disappear from the aqueous media in the course of the reaction, but they demonstrate quite a significant displacement of protons normal to the membrane plane.

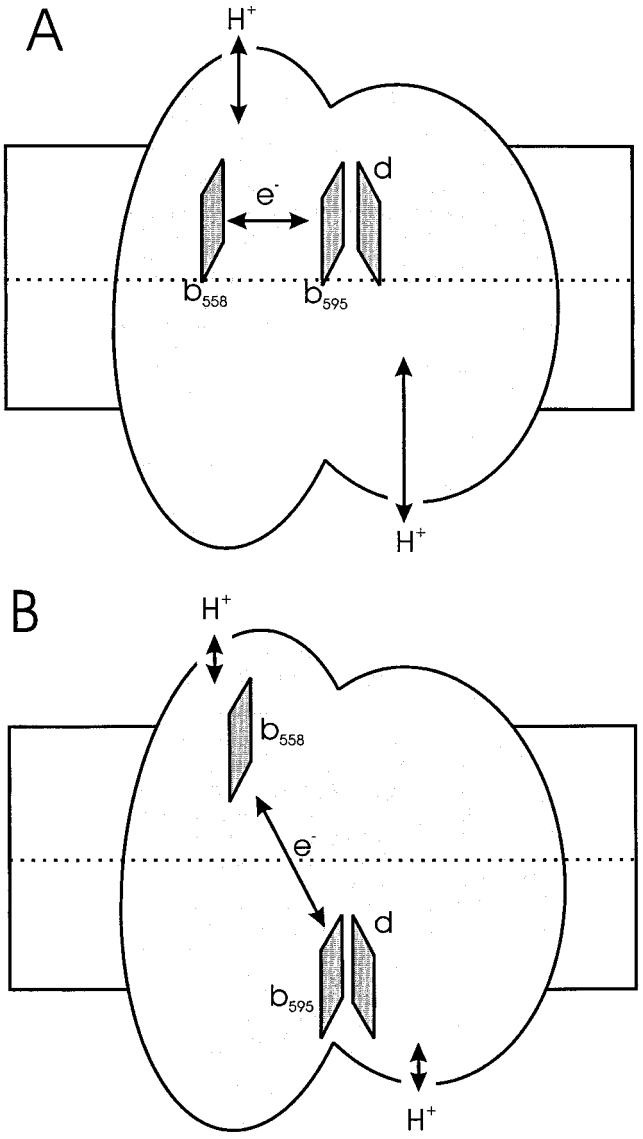

FIGURE 8: Possible mechanisms of transmembrane charge separation in cytochrome *bd* as part of the reaction with O_2 and electron backflow. (A) Vectorial proton movement. (B) Vectorial electron transfer.

The electrogenic redox-linked protonation of the oxygen-reducing center of cytochrome *bd* may be expected to involve some structural domain analogous to the input proton channel(s) of the heme−copper oxidases. The highly conserved glutamic acid residues E99 and E107, both located on transmembrane helix III inside the hydrophobic barrier, could be involved in such a structure (*7*).

*Comparison of the Electrogenic Responses Associated with the Direct and Reversed Electron Transfer***.** The absolute amplitudes of the electrogenic responses coupled to electron

transfer in the forward and reversed directions taken alone do not make it possible to determine the number of elementary charges transferred across the dielectric barrier in either direction. Some internal calibration is required for quantitative interpretation of the data (*16*, *20*, *22*). It is however possible to obtain both types of data from the same sample, and it is interesting to compare the size of the responses. Since some experimental numbers in the calculation below are small and variable, these estimates are not meant to prove any specific mechanism or model. They can provide the reader with some numbers, which would be difficult to derive without knowing details of the experiments.

In the reaction of fully reduced cytochrome *bd* with oxygen, the experimentally measured electrogenic response typically reached a maximum value of ~7 mV. Taking into account partial oxidation of cytochrome *bd* by the added oxygen prior to the flash (see Materials and Methods), we must correct this value to ~15 mV for 100% yield in the reaction. In the backflow measurements, the maximal size of the electrogenic response extrapolated to zero CO recombination rate is ~0.6 mV, that is ~5% of the flow-flash response. However, the parallel spectrophotometric measurements show that only 4−5% of heme b_{558} becomes reduced in this reaction (Figure 4). Hence, extrapolation of the electrogenic amplitude of the backflow reaction to 100% yield leads to a value 12−15 mV, very close to the maximal extrapolated value for the **R→F** transition in the flow-flash experiment. (Note that only *one* electron is transferred in the backflow experiment while in the flow-flash reaction with oxygen, *three* electrons are involved.)

Role of Heme b_{595}. The above discussion does not take into account the role of heme b_{595} in the reactions observed. Electron flow in cytochrome *bd* has been described as a linear sequence: $b_{558} \rightarrow b_{595} \rightarrow d$ (*8*). Accordingly, one could expect that electron redistribution from heme *d* to heme b_{558} in the course of electron backflow would follow the route: $b_{558} \leftarrow b_{595} \leftarrow d$. In principle, intercalation of heme b_{595} between hemes *d* and b_{558} might lead to heterogeneous kinetics of intramolecular charge translocation coupled to electron transfer between hemes b_{558} and *d* in either the forward or the reverse direction. While interpretation of the events linked to the forward electron transfer is complicated by the presence of a lag phase introduced by the oxygen binding step, the electrometric traces in the backflow experiments monitor purely intramolecular electron transfer and nevertheless reveal only a single phase in the rise of the membrane potential; neither a rapid initial jump in $\Delta\Psi$ nor a lag potentially associated with a heme *d*→heme b_{595} electron-transfer step could be resolved, despite an excellent signal-to-noise ratio and microsecond time resolution. These data together with the fact that reversed electrogenesis matches oxidation of heme *d* kinetically (Figure 5) may have some bearing on the role of heme b_{595} in intramolecular electron transfer in cytochrome *bd*. The following explanations can be briefly considered.

Heme b_{595} is not involved in the redox equilibration of heme *d* with heme b_{558}, and direct equilibration $b_{558} \leftarrow d$ takes place (e.g., there remains the possibility that heme b_{595} lies beyond heme *d* in the electron flow pathway, as in the case of Cu_B in CcO); this is a rather formal explanation but one which cannot be discarded.

Redox equilibration between hemes *d* and b_{595} is very rapid ($\tau \leq 5\ \mu s$) and nonelectrogenic. However, no evidence for a rapid phase of heme *d* oxidation upon CO photolysis could be observed spectrophotometrically (Figures 4 and 5). It is possible that, as ferric heme b_{595} is unprotonated, its transient midpoint potential on a microsecond time scale is low, as compared to the equilibrium value where the reduced state of the heme is stabilized by redox-linked protonation, and thus the reduced state of this center is never populated to a significant extent during electron backflow.

Hemes b_{558} and b_{595} are in rapid redox equilibrium, while electron transfer from heme *d* to b_{595} is relatively slow. Such a model would be in agreement with the results of recent pulse radiolysis studies (*8*). There also remains the possibility that heme b_{595} lies beyond heme *d* in the electron flow pathway, as in the case of Cu_B in CcO.

ACKNOWLEDGMENT

We are indebted to Dr. J. Osborne and Prof. R. B. Gennis for the GO105/pTK1 strain of *Escherichia coli*, to Dr. N. Yu. Safronova for growing the cells, to Matti Lehtinen for precision machining work, and to Martti Heikkenen for help with constructing equipment.

REFERENCES

1. Ferguson-Miller, S., and Babcock, G. T. (1996) *Chem. Rev. 7*, 2889−2907.
2. Poole, R. K. (1988) in *Bacterial Energy Transduction* (Anthony, C., Ed.) pp 231−291, Academic Press, London.
3. Borisov, V. B. (1996) *Biochemistry* (*Moscow*) *61*, 565−574.
4. Junemann, S. (1997) *Biochim. Biophys. Acta 1321*, 107−127.
5. Winstedt, L., Yoshida, K., Fujita, Y., and Wachenfeldt, C. V. (1998) *J. Bacteriol. 180*, 6571−6580.
6. Sakamoto, J., Koga, E., Mizuta, T., Sato, C., Noguchi, S., and Sone. (1999) *Biochim. Biophys. Acta 1411*, 147−158.
7. Osborne, J. P., and Gennis, R. B. (1999) *Biochim. Biophys. Acta 1410*, 32−50.
8. Kobayashi, K., Tagawa, S., and Mogi, T. (1999) *Biochemistry 38*, 5913−5917.
9. Puustinen, A., Finel, M., Haltia, T., Gennis, R. B., and Wikström, M. (1991) *Biochemistry 30*, 3936−3942.
10. Calhoun, M. W., Oden, K. L., Gennis, R. B., Teixeira de Mattos, M. J., and Neijssel, O. M. (1993) *J. Bacteriol. 175*, 3020−3025.
11. Bertsova, Y. V., Bogachev, A. V., and Skulachev, V. P. (1997) *FEBS Lett. 414*, 369−372.
12. Mitchell, P. (1966) *Chemiosmotic Coupling in Oxidative and Photosynthetic Phosphorylation*, Glynn Research Ltd., Bodmin, U.K.
13. Wikström, M. (1977) *Nature 266*, 271−273.
14. Koland, J. G., Miller, M. J., and Gennis, R. B. (1984) *Biochemistry 23*, 445−453.
15. Kolonay, J. F., Jr., and Maier, R. J. (1997) *J. Bacteriol. 179*, 3813−3817.
16. Zaslavsky, D., Kaulen, A., Smirnova, I. A., Vygodina, T. V., and Konstantinov, A. A. (1993) *FEBS Lett. 336*, 389−393.
17. Zaslavskiy, D. L. (1994) Mechanism of Membrane Potential Generation by Cytochrome C Oxidase. Ph.D. Thesis, Moscow State University, Moscow.
18. Zaslavsky, D. L., Smirnova, I. A., Siletsky, S. A., Kaulen, A. D., Millett, F., and Konstantinov, A. A. (1995) *FEBS Lett. 359*, 27−30.
19. Konstantinov, A. A., Siletskiy, S. A., Mitchell, D., Kaulen, A. D., and Gennis, R. B. (1997) *Proc. Natl. Acad. Sci. U.S.A. 94*, 9085−9090.
20. Siletsky, S., Kaulen, A. D., and Konstantinov, A. A. (1999) *Biochemistry 38*, 4853−4861.
21. Verkhovsky, M. I., Morgan, J. E., Verkhovskaya, M., and Wikstrom, M. (1997) *Biochim. Biophys. Acta 1318*, 6−10.

22. Jasaitis, A., Verkhovsky, M. I., Morgan, J. E., Verkhovskaya, M. L., and Wikstrom, M. (1999) *Biochemistry 38*, 2697−2706.
23. Gibson, Q. H., and Greenwood, C. (1963) *Biochem. J. 86*, 541−554.
24. Hill, B. C., Hill, J. J., and Gennis, R. B. (1994) *Biochemistry 33*, 15110−15115.
25. Hartzell, C. R., and Beinert, H. (1974) *Biochim. Biophys. Acta 368*, 318−338.
26. Baker, G. M., and Palmer, G. (1987) *Biochemistry 26*, 3038−3044.
27. Kaysser, T. M., Ghaim, J. B., Georgiou, C., and Gennis, R. B. (1995) *Biochemistry 34*, 13491−13501.
28. Miller, M. J., and Gennis, R. B. (1986) *Methods Enzymol. 126*, 138−145.
29. Borisov, V., Arutyunyan, A. M., Osborne, J. P., Gennis, R., and Konstantinov, A. A. (1999) *Biochemistry 38*, 740−750.
30. Tsubaki, M., Hori, H., Mogi, T., and Anraku, Y. (1995) *J. Biol. Chem. 270*, 28565−28569.
31. Rigaud, J.-L., Pitard, B., and Levy, D. (1995) *Biochim. Biophys. Acta 1231*, 223−246.
32. Verkhovskaya, M. L., García-Horsman, A., Puustinen, A., Rigaud, J.-L., Morgan, J. E., Verkhovsky, M. I., and Wikström, M. (1997) *Proc. Natl. Acad. Sci. U.S.A. 94*, 10128−10131.
33. Morgan, J. E., Verkhovsky, M. I., and Wikstrom, M. (1996) *Biochemistry 35*, 12235−12240.
34. Drachev, L. A., Jasaitis, A. A., Kaulen, A. D., Kondrashin, A. A., Liberman, E. A., Nemecek, I. B., Ostroumov, S. A., Semenov, A. Y., and Skulachev, V. P. (1974) *Nature 249*, 321−324.
35. Drachev, L. A., Kaulen, A. D., Semenov, A. Y., Severina, I. I., and Skulachev, V. P. (1979) *Anal. Biochem. 96*, 250−262.
36. Morgan, J. E., Verkhovsky, M. I., Puustinen, A. E., and Wikström, M. (1993) *Biochemistry 32*, 11413−11418.
37. Kahlow, M. A., Zuberi, T. M., Gennis, R. B., and Loehr, T. M. (1991) *Biochemistry 30*, 11485−11489.
38. Borisov, V., Gennis, R., and Konstantinov, A. A. (1995) *Biochem. Mol. Biol. Int. 37*, 975−982.
39. Drachev, L. A., Kaurov, B. S., Mamedov, M. D., Mulkidjanian, A. Y., Semenov, A. Y., Shinkarev, V. P., Skulachev, V. P., and Verkhovsky, M. I. (1989) *Biochim. Biophys. Acta 973*, 189−197.
40. Drachev, L. A., Kaulen, A. D., and Skulachev, V. P. (1978) *FEBS Lett. 87*, 161−167.
41. Siletsky, S. A., Kaulen, A. D., and Konstantinov, A. A. (1997) *Eur. J. Biophys. 26*, 98.
42. Wrigglesworth, J. (1984) *Biochem. J. 217*, 715−719.
43. Orii, Y. (1988) *Ann. N.Y. Acad. Sci. 550*, 105−117.
44. Vygodina, T., and Konstantinov, A. (1989) *Biochim. Biophys. Acta 973*, 390−398.
45. Weng, L., and Baker, G. M. (1991) *Biochemistry 30*, 5727−5733.
46. Fabian, M., and Palmer, G. (1995) *Biochemistry 34*, 13802−13810.
47. Lorence, R. M., and Gennis, R. B. (1989) *J. Biol. Chem. 264*, 7135−7140.
48. Borisov, V. B., Gennis, R. B., and Konstantinov, A. A. (1995) *Biochemistry* (*Moscow*) *60*, 231−239.
49. Vygodina, T. V., and Konstantinov, A. A. (1988) *Ann. N.Y. Acad. Sci. 550*, 124−138.
50. Brittain, T., Little, R. H., Greenwood, C., and Watmough, N. J. (1996) *FEBS Lett. 399*, 21−25.
51. Moody, A. J., Rumbley, J. N., Ingledew, W. J., Gennis, R. B., and Rich, P. R. (1993) *Biochem. Soc. Trans. 21*, 255.
52. Watmough, N. J., Cheesman, M. R., Greenwood, C., and Thomson, A. J. (1994) *Biochem. J. 300*, 469−475.
53. Moody, A. J., and Rich, P. R. (1994) *Eur. J. Biochem. 226*, 731−737.
54. Morgan, J. E., Verkhovsky, M. I., Puustinen, A., and Wikström, M. (1995) *Biochemistry 34*, 15633−15637.
55. Boelens, R., Wever, R., and Van Gelder, B. F. (1982) *Biochim. Biophys. Acta 682*, 264−272.
56. Brzezinski, P. (1996) *Biochemistry 35*, 5611−5615.
57. Oliveberg, M., and Malmström, B. G. (1991) *Biochemistry 30*, 7053−7057.
58. Verkhovsky, M. I., Morgan, J. E., and Wikström, M. (1992) *Biochemistry 31*, 11860−11863.
59. Hallén, S., Brzezinski, P., and Malmström, B. G. (1994) *Biochemistry 33*, 1467−1472.
60. Junemann, S., Wrigglesworth, J. M., and Rich, P. R. (1997) *Biochemistry 36*, 9323−9331.
61. Koland, J. G., Miller, M. J., and Gennis, R. B. (1984) *Biochemistry 23*, 1051−1056.
62. Wikström, M., Krab, K., and Saraste, M. (1981) *Cytochrome Oxidase−A Synthesis*, Academic Press, New York.
63. Konstantinov, A. (1998) *J. Bioenerg. Biomembr. 30*, 121−130.
64. Varotsis, C., Zhang, Y., Appelman, E. H., and Babcock, G. T. (1993) *Proc. Natl. Acad. Sci. U.S.A. 90*, 237−241.
65. Babcock, G. T., and Varotsis, C. (1993) *J. Bioenerg. Biomembr. 25*, 71−80.
66. Iwata, S., Ostermeier, C., Ludwig, B., and Michel, H. (1995) *Nature 376*, 660−669.
67. Tsukihara, T., Aoyama, H., Yamashita, E., Takashi, T., Yamaguichi, H., Shinzawa-Itoh, K., Nakashima, R., Yaono, R., and Yoshikawa, S. (1996) *Science 272*, 1136−1144.
68. Lorence, R. M., Carter, K., Gennis, R. B., Matsushita, K., and Kaback, H. R. (1988) *J. Biol. Chem. 11*, 5271−5276.
69. Mitchell, P. (1968) *Chemiosmotic Coupling and Energy Trunsduction*, Glynn Research Ltd., Bodmin.

BI001165N